

This discussion paper is/has been under review for the journal Atmospheric Chemistry and Physics (ACP). Please refer to the corresponding final paper in ACP if available.

Evidence for ambient dark aqueous SOA formation in the Po Valley, Italy

A. P. Sullivan¹, N. Hodas², B.J. Turpin³, K. Skog⁴, F. N. Keutsch^{4,5}, S. Gilardoni⁶, M. Paglione⁶, M. Rinaldi⁶, S. Decesari⁶, M. C. Facchini⁶, L. Poulain⁷, H. Herrmann⁷, A. Wiedensohler⁷, E. Nemitz⁸, M. M. Twigg⁸, and J. L. Collett Jr.¹

¹Colorado State University, Department of Atmospheric Science, Fort Collins, CO 80523, USA

²California Institute of Technology, Division of Chemical Engineering, Pasadena, CA 91125, USA

³Rutgers University, Department of Environmental Sciences, New Brunswick, NJ 08901, USA

⁴University of Wisconsin – Madison, Department of Chemistry, Madison, WI 53706, USA

⁵Harvard University, Department of Chemistry and Chemical Biology, Cambridge, MA 02138, USA

⁶Istituto di Scienze dell'Atmosfera e del Clima, Consiglio Nazionale delle Ricerche, 40129 Bologna, Italy

⁷Leibniz Institute for Tropospheric Research, 04318 Leipzig, Germany

⁸Centre for Ecology and Hydrology, Bush Estate, Penicuik, EH26QB, UK

Evidence for ambient
dark aqueous SOA
formation in the Po
Valley, Italy

A. P. Sullivan et al.

Title Page

Abstract

Introduction

Conclusions

References

Tables

Figures



Back

Close

Full Screen / Esc

Printer-friendly Version

Interactive Discussion



Received: 31 October 2015 – Accepted: 24 November 2015 – Published: 16 December 2015

Correspondence to: A. P. Sullivan (sullivan@atmos.colostate.edu)

Published by Copernicus Publications on behalf of the European Geosciences Union.

Discussion Paper | Discussion Paper | Discussion Paper | Discussion Paper | Discussion Paper

ACPD

15, 35485–35521, 2015

**Evidence for ambient
dark aqueous SOA
formation in the Po
Valley, Italy**

A. P. Sullivan et al.

Title Page

Abstract

Introduction

Conclusions

References

Tables

Figures



Back

Close

Full Screen / Esc

Printer-friendly Version

Interactive Discussion



Abstract

Laboratory experiments suggest that water-soluble products from the gas-phase oxidation of volatile organic compounds can partition into atmospheric waters where they are further oxidized to form low volatility products, providing an alternative route for oxidation in addition to further oxidation in the gas-phase. These products can remain in the particle phase after water evaporation forming what is termed as aqueous secondary organic aerosol (aqSOA). However, few studies have attempted to observe ambient aqSOA. Therefore, a suite of measurements, including near real-time WSOC (water-soluble organic carbon), inorganic anions/cations, organic acids, and gas-phase glyoxal, were made during the PEGASOS (Pan-European Gas-AeroSols-climate interaction Study) 2012 campaign in the Po Valley, Italy to search for evidence of aqSOA. Our analysis focused on two specific periods: Period A on 19–21 June and Period B on 3–5 July to represent the first and second halves of the study, respectively. The large scale circulation was predominately from the west in both periods. Plus back trajectory analysis suggested all sites sampled similar air masses during both periods allowing for comparison of Periods A and B. The data collected during both periods were divided into times of increasing relative humidity (RH) and decreasing RH with the aim of diminishing the influence of dilution and mixing on SOA concentrations and other measured variables. Evidence for local aqSOA formation was only observed during Period A. When this occurred, there was a correlation of WSOC with organic aerosol ($R^2 = 0.86$), aerosol liquid water ($R^2 = 0.69$), RH ($R^2 = 0.45$), and aerosol nitrate ($R^2 = 0.71$). Additionally, this was only observed during times of increasing RH, which coincided with dark conditions. Comparisons of WSOC with oxygenated organic aerosol (OOA) factors determined from application of positive matrix factorization analysis on the aerosol mass spectrometer observations of the submicron non-refractory organic particle composition suggested that the WSOC in Periods A and B differed (Period A WSOC vs. OOA-2 $R^2 = 0.85$ and OOA-4 $R^2 = 0.03$ whereas Period B WSOC vs. OOA-2 $R^2 = 0.03$ and OOA-4 $R^2 = 0.64$). OOA-2 had a high O/C (oxygen/carbon) ratio of 0.77, provid-

Evidence for ambient dark aqueous SOA formation in the Po Valley, Italy

A. P. Sullivan et al.

Title Page

Abstract

Introduction

Conclusions

References

Tables

Figures



Back

Close

Full Screen / Esc

Printer-friendly Version

Interactive Discussion



and July 2012, focusing on the Po Valley. PEGASOS was a European wide study to address regional to global feedbacks between atmospheric chemistry and climate in different locations as well as in the laboratory. The observations included airborne measurements using a Zeppelin and multiple ground sites to study surface–atmosphere exchange, assess the vertical structure of the atmosphere, and study boundary layer photochemistry. An auxiliary site was located in Bologna. Our measurements were made at the main ground site in San Pietro Capofiume (SPC, Fig. 1). The SPC field station is located approximately 40 km northeast of Bologna and 30 km south of the Po River in flat terrain of agricultural fields (Fig. 1c and d).

Our measurements included running a Particle-into-Liquid Sampler – Ion Chromatography (PILS-IC) (Orsini et al., 2003) system for inorganic cations, inorganic anions, and light organic acids and a Particle-into-Liquid Sampler – Total Organic Carbon (PILS-TOC) system (Sullivan et al., 2004) for particle-phase WSOC. A PILS collects the ambient particles into purified water, providing the liquid sample for analysis. Both systems operated at 15 L min^{-1} with a $2.5 \mu\text{m}$ size-cut cyclone. Two annular denuders coated with sodium carbonate and phosphorous acid to remove inorganic gases were placed upstream of the PILS-IC and for the PILS-TOC an upstream activated carbon parallel plate denuder (Eatough et al., 1993) was used to remove organic gases. In addition, for the PILS-TOC, a normally open actuated valve controlled by an external timer was periodically closed every 2 h for 30 min forcing the airflow through a Teflon filter before entering the PILS. This was to allow for a real background measurement to be determined. Ambient $\text{PM}_{2.5}$ WSOC concentrations were calculated as the difference between the filtered and non-filtered measurements. The background was assumed to be constant between consecutive background measurements. Based on comparison with integrated quartz filter WSOC measurements, it appears the difference between filtered and non-filtered measurements was being overestimated by $\sim 20\%$ before the carbon denuder was switched out on 25 June. Therefore, the WSOC concentrations before this date have been corrected for this.

Evidence for ambient dark aqueous SOA formation in the Po Valley, Italy

A. P. Sullivan et al.

Title Page

Abstract

Introduction

Conclusions

References

Tables

Figures



Back

Close

Full Screen / Esc

Printer-friendly Version

Interactive Discussion



Evidence for ambient dark aqueous SOA formation in the Po Valley, Italy

A. P. Sullivan et al.

Title Page

Abstract

Introduction

Conclusions

References

Tables

Figures



Back

Close

Full Screen / Esc

Printer-friendly Version

Interactive Discussion



For the PILS-IC, the liquid sample from the PILS was split between two Dionex ICS-1500 ion chromatographs. These systems include an isocratic pump, self-regenerating anion or cation SRS-ULTRA suppressor, and conductivity detector. The cations were separated using a Dionex IonPac CS12A analytical (4 × 250 mm) column with eluent of 18 mM methanesulfonic acid at a flowrate of 1.0 mL min⁻¹. A Dionex IonPac AS15 analytical (4 × 250 mm) column employing an eluent of 38 mM sodium hydroxide at a flowrate of 1.5 mL min⁻¹ was used for the anion analysis. A new chromatogram was obtained every 30 min with a sample loop fill time of 8 min. The limit of detection (LOD) for the various anions and cations was approximately 0.02 µg m⁻³. These inorganic PILS data were also used to determine ALW from the Extended Aerosol Inorganics Model (E-AIM; Wexler and Clegg, 2002) run in a metastable state. More information on the ALW calculations can be found in Hodas et al. (2014).

In the PILS-TOC, the liquid sample obtained from the PILS was pushed through a 0.2 µm PTFE liquid filter by a set of syringe pumps to ensure any insoluble particles were removed. The flow was then directed into a Sievers Model 800 Turbo TOC (Total Organic Carbon) Analyzer. This analyzer works by converting the organic carbon in the liquid sample to carbon dioxide through chemical oxidation involving ammonium persulfate and ultraviolet light. The conductivity of the dissolved carbon dioxide formed is determined. The amount of organic carbon in the liquid sample is proportional to the measured increase in conductivity. The analyzer was run in on-line mode providing a 6 min integrated measurement of WSOC with a LOD of 0.1 µg C m⁻³.

Other measurements presented here include 2.5 min integrated organic aerosol (OA) concentrations determined by a High Resolution – Time-of-Flight Aerosol Mass Spectrometer (HR-ToF-AMS) (Drewnick et al., 2005; DeCarlo et al., 2006; Canagaratna et al., 2007). Positive matrix factorization (PMF) analysis of the AMS OA data was performed using the Multilinear Engine algorithm (ME-2) (Paatero, 1999) implemented within the toolkit Solution Finder (SoFi) developed by Canonaco et al. (2013). More details on the AMS ME-2 analysis can be found in the Supplement. Gas-phase glyoxal was determined by the Madison Laser-Induced Phosphorescence (Mad-LIP) in-

Evidence for ambient dark aqueous SOA formation in the Po Valley, Italy

A. P. Sullivan et al.

Title Page

Abstract

Introduction

Conclusions

References

Tables

Figures

◀

▶

◀

▶

Back

Close

Full Screen / Esc

Printer-friendly Version

Interactive Discussion



relationship with RH. Only during the times of increasing RH did Period A have a relationship of increasing WSOC with RH, consistent with local aqSOA formation. This can further be illustrated by examining the correlation of WSOC vs. organic aerosol (OA), aerosol liquid water (ALW), and RH for Periods A and B during the times of RH increasing (Fig. 4). In both periods during the time of RH increasing, WSOC had a strong relationship with OA (Period A $R^2 = 0.86$ and Period B $R^2 = 0.66$), but only Period A additionally had a correlation of the WSOC with both ALW and RH. The good correlation between WSOC and ALW is in agreement with a previous smog chamber study that found that ALW is a key determinant of SOA yield (Zhou et al., 2011). This also supports a recent study that observed ambient aqSOA formation during the nighttime as evident by the increased partitioning of gas-phase WSOC to the particle-phase with increasing RH (El-Sayed et al., 2015).

Figure 5 shows the correlation of WSOC vs. nitrate, oxalate, and sulfate for the times of RH increasing. Nitrate and WSOC are strongly correlated only during the times of RH increasing for Period A (Period A $R^2 = 0.71$ vs. Period B $R^2 = 0.18$). This likely reflects the difference in ALW in the two periods as well since nitrate drives ALW concentrations (Hodas et al., 2014). Early morning nitrate peaks were observed at SPC during the first part of the study, but were absent at the upwind Bologna site (Fig. 6). The occurrence of these peaks overlaps with Period A. (Note, the nitrate event observed on 6 and 7 July will be discussed in Sect. 3.4.) This additionally suggested that the nitrate formation or the ammonium-nitrate-ammonia-nitric acid equilibrium at SPC was locally controlled since the back trajectory analysis indicated both the SPC and Bologna sites were sampling similar upwind air masses (Fig. 1). Therefore, the correlation with locally formed particulate nitrate suggests local formation of WSOC. (Note, increased nitrate also results in higher ALW at the same RH.) This argues that aqSOA formation was predominately local during Period A.

To help better understand the potential for aqSOA formation, correlations with oxalate and sulfate can be examined. Oxalate and sulfate are known tracers for aerosol formation through cloud processing (Sorooshian et al., 2010), although sulfate does

volatility types (OOA-2, OOA-3, and OOA-4). More details on the AMS ME-2 analysis can be found in the Supplement.

As shown in Fig. 8, the measured WSOC from the first half of the study is dominated by OOA-2 and the second half by OOA-4. This can be further illustrated by looking at the correlation of WSOC vs. OOA-2 and OOA-4 during the times of RH increasing for Periods A and B (Fig. 9). The WSOC in Period A is most strongly correlated with OOA-2 ($R^2 = 0.85$) and in Period B with OOA-4 ($R^2 = 0.64$).

To estimate how each AMS ME-2 factor contributed to WSOC and what fraction of each factor was water-soluble, a multilinear regression analysis was tentatively performed using the method proposed by Timonen et al. (2013). The results are shown in Table 3 and Fig. 10. This approach seeks to reproduce the total WSOC as a linear combination of the different factors, whilst minimizing the residuals and, unlike in Timonen et al. (2013), capping the individual factor contributions at 1 to allow conservation of the carbon mass. The regression analysis was carried out with a zero intercept like in Timonen et al. (2013), as well as with a non-zero intercept to account for possible instrumental biases between the AMS and PILS methods. Only the four OOA factors were considered, while HOA was assumed to be completely insoluble. All concentrations are in carbon mass units, which for the AMS factors were derived from organic mass concentrations through factor-specific OM/OC ratios. The results of the regression are reported for the whole PILS measurement period and also for Periods A and B separately.

The results for the whole measurement period indicate that the largest contributions to the WSOC must be attributed to the OOA types which were simply the most abundant (OOA-3 and OOA-4), but the water-soluble fractions as reflected in the regression coefficients were greatest for OOA-2 and OOA-4 in agreement with their high correlation coefficients with WSOC. Interestingly, OOA-2 and OOA-4 are also the factors possessing the highest O/C ratios (0.77 and 0.76, respectively), with respect to the other two (O/C = 0.48 for OOA-1 and 0.36 for OOA-3). Therefore, in this study the

Evidence for ambient dark aqueous SOA formation in the Po Valley, Italy

A. P. Sullivan et al.

Title Page

Abstract

Introduction

Conclusions

References

Tables

Figures



Back

Close

Full Screen / Esc

Printer-friendly Version

Interactive Discussion



factor-specific WSOC fractions seem related to the oxygen contents measured by the AMS.

The multilinear regression analysis performed on the Period A measurements suggests that the largest water-soluble fractions are exhibited by OOA-1 and OOA-2, whose concentrations were observed to increase along with RH and WSOC for all the days in this period of the campaign. Due to the very different absolute average concentrations, the second factor (OOA-2) provided the largest contribution to WSOC, accounting for more than one third of the total water-soluble carbon concentration. Interestingly, the diurnal trend of OOA-1 indicated that its partitioning to the aerosol phase was largely reversible, and its concentrations declined steeply in the late morning hours when RH and ALW decreased. This can be illustrated by the additional correlation of WSOC with OOA-1 during the times of RH increasing for only Period A (Fig. 9a, $R^2 = 0.50$). This is not surprising given the high correlation between OOA-1 and nitrate, which drives ALW in this region, during the whole measurement period ($R^2 = 0.64$). In the same hours of the day, the OOA-2 concentrations were largely unaffected by RH indicating (a) that OOA-2 mainly accounted for oxidized compounds stable in the aerosol phase and (b) that boundary layer growth is not the reason for the decrease in OOA-1 as this should have affected all factors. OOA-1 and OOA-2 can therefore be interpreted as two aging stages of aqSOA formation during Period A.

The results obtained for Period B show again that the greatest coefficients (hence the largest water-soluble fractions) were found for OOA-2 and OOA-4. However, due to its very small concentrations in this period, OOA-2 provided a negligible contribution to WSOC (1 %), while OOA-4 was estimated to account for more than half of the WSOC carbon content. The examination of time trends indicates that OOA-4 is mainly a background component of the aerosol, showing no appreciable increase at the time when RH increased for a few hours on the mornings of 5 and 6 July. Similar to Period A, here again the times when RH and ALW were high showed relatively high concentrations of OOA-1, which represented an additional (though small compared to OOA-4) contribution to WSOC.

Evidence for ambient dark aqueous SOA formation in the Po Valley, Italy

A. P. Sullivan et al.

Title Page	
Abstract	Introduction
Conclusions	References
Tables	Figures
◀	▶
◀	▶
Back	Close
Full Screen / Esc	
Printer-friendly Version	
Interactive Discussion	



Evidence for ambient dark aqueous SOA formation in the Po Valley, Italy

A. P. Sullivan et al.

Title Page

Abstract

Introduction

Conclusions

References

Tables

Figures



Back

Close

Full Screen / Esc

Printer-friendly Version

Interactive Discussion



ilar to those of Period A were observed at SPC. Interestingly, the nitrate observed on these days was also observed in Bologna (Fig. 6). The timing of the peak nitrate concentration also differed from Period A; it occurred later in the morning, around 07:00 LT, whereas during Period A nitrate peaked around midnight or 01:00 LT and then again around 07:00 LT. This suggests that the presence and timing of elevated nitrate, which is a strong determinant of ALW, may be important for local aqSOA production and resulting WSOC aerosol concentrations in this region.

An examination of possible gas-phase precursors (e.g., aromatic VOCs and glyoxal, Table 1) shows no noticeable decline in concentration from the first to second half of the measurement period. Therefore, a possible explanation for the difference between Periods A and B is meteorology. Period A featured an anticyclonic condition that led to air stagnation; Period B featured stronger transport and ventilation. Therefore, during Period B intermediate products needed to form appreciable concentrations of aqSOA are less likely to quickly accumulate in the local boundary layer.

It is possible that another key ingredient in the chemistry is ammonia. Recent studies have suggested possible aqSOA formation processes mediated by ammonia and other atmospheric bases (Galloway et al., 2009; Nozière et al., 2009; Ortiz-Montalvo et al., 2014; Yu et al., 2011). Ammonia is prevalent in the Po Valley due to agricultural activities. During Period A, high ammonia concentrations (greater than $\sim 30 \mu\text{g m}^{-3}$) were observed only at SPC (Fig. 11a).

Overall, the data suggest that local aqSOA production during the stagnation of Period A is not due to cloud processing. Our results also suggest that this aqueous chemistry occurs in the dark, which likely provides the favorable low temperatures and high RH for nitrate aerosol and ALW (Hodas et al., 2014). Based on other measurements at SPC, the stagnation conditions and elevated nitrate around midnight occurred each day from 14 June through 23 June, suggesting that the local aqSOA formation actually commenced five days earlier. When all these conditions were met, each day $\sim 1 \mu\text{g C m}^{-3}$ of new WSOC (determined as the change in WSOC concentration during the times of RH increasing) can be attributed to this process.

4 Summary

Measurements were conducted during the PEGASOS Study in the Po Valley of Italy during June and July 2012 in San Pietro Capofiume (SPC). The goal was to look for evidence of aqSOA in the ambient atmosphere. Measurements included near real-time WSOC (a good proxy for SOA), inorganic anions/cations, and organic acids. The data were analyzed in terms of the times when RH increased from 40 to 80 % (times of RH increasing) and then when the RH decreased from 80 back to 40 % (times of RH decreasing) in order to diminish influences from dilution and mixing on ambient measurements. The analysis focused on two periods: Period A on 19–21 June and Period B on 3–5 July.

Evidence for local aqSOA formation in wet aerosols was observed during Period A. When this occurred there was a correlation of WSOC with OA, ALW, RH, and nitrate. Additionally, this was only observed during times of RH increasing, suggesting the aqSOA was formed in the dark. The aqSOA formation is thought to be local because elevated nitrate, the driver for aerosol water, was only observed at the main ground site in SPC even though the auxiliary site in Bologna was sampling similar upwind air masses at the time.

Period B differed from Period A. The WSOC during Period B was likely formed regionally. Interestingly, during Period B as well as Period A a correlation was found between oxalate and sulfate. This suggests that oxalate concentrations were not strongly affected by local aqSOA formation. More importantly, it indicates that oxalate is not a good universal marker for aqSOA. It is probably better for observing aqSOA produced in clouds, which were present west of SPC only in Period B.

A comparison of WSOC with the AMS PMF OOA factors showed that Period A featured high O/C ratios, consistent with aqSOA formation. However, they also reinforce the conclusion that the composition of the WSOC differed between Periods A and B. Periods A and B were dominated by two different OOA factors, OOA-2 (locally produced) and OOA-4 (long-range transported), respectively.

Evidence for ambient dark aqueous SOA formation in the Po Valley, Italy

A. P. Sullivan et al.

Title Page

Abstract

Introduction

Conclusions

References

Tables

Figures



Back

Close

Full Screen / Esc

Printer-friendly Version

Interactive Discussion



Evidence for ambient dark aqueous SOA formation in the Po Valley, Italy

A. P. Sullivan et al.

[Title Page](#)[Abstract](#)[Introduction](#)[Conclusions](#)[References](#)[Tables](#)[Figures](#)[Back](#)[Close](#)[Full Screen / Esc](#)[Printer-friendly Version](#)[Interactive Discussion](#)

reversibility of uptake under dark and irradiated conditions, *Atmos. Chem. Phys.*, 9, 3331–3345, doi:10.5194/acp-9-3331-2009, 2009.

Gaston, C. J., Riedel, T. P., Zhang, Z., Gold, A., Surratt, J. D., and Thornton, J. A.: Reactive uptake of an isoprene-derived epoxydiol to submicron aerosol particles, *Environ. Sci. Technol.*, 48, 11178–11186, 2014.

Heald, C. L., Jacob, D. J., Park, R. J., Russell, L. M., Huebert, B. J., Seinfeld, J. H., Liao, H., and Weber, R. J.: A large organic aerosol source in the free troposphere missing from current models, *Geophys. Res. Lett.*, 32, L18809, doi:10.1029/2005GL023831, 2005.

Hennigan, C. J., Bergin, M. H., Dibb, J. E., and Weber, R. J.: Enhanced secondary organic aerosol formation due to water uptake by fine particles, *Geophys. Res. Lett.*, 35, L18801, doi:10.1029/2008GL035046, 2008.

Hodas, N., Sullivan, A. P., Skog, K., Keutsch, F. N., Collett Jr., J. L., Decesari, S., Facchini, M. C., Carlton, A. G., Laaksonen, A., and Turpin, B. J.: Aerosol liquid water driven by anthropogenic nitrate: implications for lifetimes of water-soluble organic gases and potential for secondary aerosol formation, *Environ. Sci. Technol.*, 48, 11127–11136, 2014.

Huisman, A. J., Hottle, J. R., Coens, K. L., DiGangi, J. P., Galloway, M. M., Kammrath, A., and Keutsch, F. N.: Laser-induced phosphorescence for the in situ detection of glyoxal at part per trillion mixing ratios, *Anal. Chem.*, 80, 5884–5891, 2008.

Kanakidou, M., Seinfeld, J. H., Pandis, S. N., Barnes, I., Dentener, F. J., Facchini, M. C., Van Dingenen, R., Ervens, B., Nenes, A., Nielsen, C. J., Swietlicki, E., Putaud, J. P., Balkanski, Y., Fuzzi, S., Horth, J., Moortgat, G. K., Winterhalter, R., Myhre, C. E. L., Tsigaridis, K., Vignati, E., Stephanou, E. G., and Wilson, J.: Organic aerosol and global climate modelling: a review, *Atmos. Chem. Phys.*, 5, 1053–1123, doi:10.5194/acp-5-1053-2005, 2005.

Kondo, Y., Miyazaki, Y., Takegawa, N., Miyakawa, T., Weber, R. J., Jimenez, J. L., Zhang, Q., and Worsnop, D. R.: Oxygenated and water-soluble organic aerosols in Tokyo, *J. Geophys. Res.*, 112, D01203, doi:10.1029/2006JD007056, 2007.

Lim, Y. B., Tan, Y., Perri, M. J., Seitzinger, S. P., and Turpin, B. J.: Aqueous chemistry and its role in secondary organic aerosol (SOA) formation, *Atmos. Chem. Phys.*, 10, 10521–10539, doi:10.5194/acp-10-10521-2010, 2010.

Lambe, A. T., Onasch, T. B., Massoli, P., Croasdale, D. R., Wright, J. P., Ahern, A. T., Williams, L. R., Worsnop, D. R., Brune, W. H., and Davidovits, P.: Laboratory studies of the chemical composition and cloud condensation nuclei (CCN) activity of secondary or-

Evidence for ambient dark aqueous SOA formation in the Po Valley, Italy

A. P. Sullivan et al.

Title Page

Abstract

Introduction

Conclusions

References

Tables

Figures

◀

▶

◀

▶

Back

Close

Full Screen / Esc

Printer-friendly Version

Interactive Discussion



ganic aerosol (SOA) and oxidized primary organic aerosol (OPOA), *Atmos. Chem. Phys.*, 11, 8913–8928, doi:10.5194/acp-11-8913-2011, 2011.

Miyazaki, Y., Kondo, Y., Takegawa, N., Komazaki, Y., Kawamura, K., Mochida, M., Okuzawa, K., and Weber, R. J.: Time-resolved measurements of water-soluble organic carbon in Tokyo, *J. Geophys. Res.*, 111, D23206, doi:10.1029/2006JD007125, 2006.

Monge, M. E., Rosenørn, T., Favez, O., Müller, M., Adler, G., Riziq, A. A., Rudich, Y., Herrmann, H., George, C., and D'Anna, B.: Alternative pathway for atmospheric particles growth, *P. Natl. Acad. Sci. USA*, 109, 6840–6844, doi:10.1073/pnas.1120593109, 2012.

Nguyen, T. B., Lee, P. B., Updyke, K. M., Bones, D. L., Laskin, J., Laskin, A., and Nizkorodov, S. A.: Formation of nitrogen- and sulfur-containing light-absorbing compounds accelerated by evaporation of water from secondary organic aerosols, *J. Geophys. Res.*, 117, D01207, doi:10.1029/2011JD016944, 2012.

Nozière, B., Dziedzic, P., and Córdoba, A.: Products and kinetics of the liquid-phase reaction of glyoxal catalyzed by ammonium ions (NH_4^+), *J. Phys. Chem. A*, 113, 231–237, 2009.

Orsini, D. A., Ma, Y., Sullivan, A., Sierau, B., Baumann, K., and Weber, R. J.: Refinements to the particle-into-liquid sampler (PILS) for ground and airborne measurements of water-soluble aerosol composition, *Atmos. Environ.*, 37, 1243–1259, 2003.

Ortiz-Montalvo, D. L., Häkkinen, S. A. K., Schwier, A. N., Lim, Y. B., McNeill, V. F., and Turpin, B. J.: Ammonium addition (and aerosol pH) has a dramatic impact on the volatility and yield of glyoxal secondary organic aerosol, *Environ. Sci. Technol.*, 48, 255–262, 2014.

Paatero, P.: The multilinear engine – a table-driven, least squares program for solving multilinear problems, including the n-way parallel factor analysis model, *J. Comput. Graph. Stat.*, 8, 854–888, 1999.

Perri, M. J., Lim, Y. B., Seitzinger, S. P., and Turpin, B. J.: Organosulfates from glycolaldehyde in aqueous aerosols and clouds: laboratory studies, *Atmos. Environ.*, 44, 2658–2664, 2010.

Rolph, G. D.: Real-time Environmental Applications and Display sYstem (READY) website, available at: <http://www.arl.noaa.gov/ready/hysplit4.html> (last access: 5 August 2013), NOAA Air Resources Laboratory, Silver Spring, MD, 2013.

Seinfeld, J. H. and Pandis, S. N.: *Atmospheric Chemistry and Physics: From Air Pollution to Climate Change*, John Wiley, Hoboken, NJ, 2006.

Seinfeld, J. H. and Pankow, J. F.: Organic atmospheric particulate material, *Annu. Rev. Phys. Chem.*, 54, 121–140, 2003.

Evidence for ambient dark aqueous SOA formation in the Po Valley, Italy

A. P. Sullivan et al.

[Title Page](#)[Abstract](#)[Introduction](#)[Conclusions](#)[References](#)[Tables](#)[Figures](#)[⏪](#)[⏩](#)[◀](#)[▶](#)[Back](#)[Close](#)[Full Screen / Esc](#)[Printer-friendly Version](#)[Interactive Discussion](#)

Wexler, A. S. and Clegg, S. L.: Atmospheric aerosol models for systems including the ions H^+ , NH_4^+ , Na^+ , SO_4^{2-} , NO_3^- , Cl^- , Br^- , and H_2O , J. Geophys. Res., 107, 4207, doi:10.1029/2001JD000451, 2002.

5 Yu, G., Bayer, A. R., Galloway, M. M., Korshavn, K. J., Fry, C. G., and Keutsch, F. N.: Glyoxal in aqueous ammonium sulfate solutions: products, kinetics, and hydration effects, Environ. Sci. Technol., 45, 6336–6342, 2011.

Zhang, X., Liu, J., Parker, E. T., Hayes, P. L., Jimenez, J. L., de Gouw, J. A., Flynn, J. H., Grossberg, N., Lefer, B. L., and Weber, R. J.: On the gas-particle partitioning of soluble organic aerosol in two urban atmospheres with contrasting emissions: 1. Bulk water-soluble organic carbon, J. Geophys. Res., 117, D00V16, doi:10.1029/2012JD017908, 2012.

10 Zhou, Y., Zhang, H., Parikh, H. M., Chen, E. H., Rattanavaraha, W., Rosen, E. P., Wang, W., and Kamens, R. M.: Secondary organic aerosol formation from xylenes and mixtures of toluene and xylenes in an atmospheric urban hydrocarbon mixture: water and particle seed effects (II), Atmos. Environ., 45, 3882–3890, 2011.

Evidence for ambient dark aqueous SOA formation in the Po Valley, Italy

A. P. Sullivan et al.

Title Page

Abstract

Introduction

Conclusions

References

Tables

Figures



Back

Close

Full Screen / Esc

Printer-friendly Version

Interactive Discussion



Table 1. Average concentrations of aerosol and gas-phase species along with various meteorological parameters observed during the times of RH increasing and decreasing during Periods A and B at SPC.

	OA ($\mu\text{g m}^{-3}$)	WSOC ($\mu\text{g C m}^{-3}$)	Glycolate ($\mu\text{g m}^{-3}$)	Acetate ($\mu\text{g m}^{-3}$)	Formate ($\mu\text{g m}^{-3}$)	Chloride ($\mu\text{g m}^{-3}$)	Sulfate ($\mu\text{g m}^{-3}$)	Oxalate ($\mu\text{g m}^{-3}$)	Nitrate ($\mu\text{g m}^{-3}$)
Period A RH Increasing	8.93	4.73	0.28	0.40	0.43	0.13	3.49	0.24	2.91
Period A RH Decreasing	9.63	5.09	0.30	0.33	0.47	0.17	3.23	0.23	5.61
Period B RH Increasing	2.05	1.55	0.24	0.28	0.23	0.11	2.80	0.13	1.18
Period B RH Decreasing	2.01	1.54	0.22	0.32	0.23	0.10	2.75	0.12	1.28
	Ozone ($\mu\text{g m}^{-3}$)	NO _x ($\mu\text{g m}^{-3}$)	SO ₂ (ppb)	Benzene ($\mu\text{g m}^{-3}$)	Toluene ($\mu\text{g m}^{-3}$)	Xylene ($\mu\text{g m}^{-3}$)	Glyoxal (ppb)	T (°C)	RH (%)
Period A RH Increasing	47.42	28.90	0.65	0.21	1.21	0.26	0.05	24.47	64.49
Period A RH Decreasing	63.70	17.75	1.14	0.27	1.78	0.34	0.09	26.09	57.66
Period B RH Increasing	61.29	9.72	0.40	0.17	1.18	0.40	0.05	23.31	60.60
Period B RH Decreasing	75.40	8.08	0.51	0.17	1.11	0.44	0.07	25.02	53.88

Table 2. Equations for each of the linear regression plots shown in Figs. 4, 5, 7, and 9. Uncertainties with the least square regressions are one standard deviation.

Figure	Linear Regression Equation
4a	$y = 0.476x \pm 0.039 - 0.345 \pm 0.357$
4b	$y = 0.614x \pm 0.084 + 0.300 \pm 0.177$
4c	$y = 0.167x \pm 0.023 + 2.825 \pm 0.174$
4d	$y = 0.183x \pm 0.108 + 0.962 \pm 0.321$
4e	$y = 0.047x \pm 0.010 + 0.898 \pm 0.687$
4f	$y = -0.003x \pm 0.010 + 1.711 \pm 0.595$
5a	$y = 0.469x \pm 0.060 + 2.574 \pm 0.192$
5b	$y = 0.824x \pm 0.441 + 0.512 \pm 0.527$
5c	$y = 9.024x \pm 3.560 + 1.753 \pm 0.872$
5d	$y = 22.095x \pm 2.990 - 1.354 \pm 0.387$
5e	$y = 0.297x \pm 0.187 + 2.902 \pm 0.667$
5f	$y = 0.276x \pm 0.124 + 0.718 \pm 0.354$
7a	Period A $y = 0.040x \pm 0.007 + 0.097 \pm 0.025$ Period B $y = 0.014x \pm 0.004 + 0.090 \pm 0.012$
7b	Period A $y = 0.078x \pm 0.020 - 0.021 \pm 0.068$ Period B $y = 0.043x \pm 0.007 + 0.006 \pm 0.020$
7c	Period A $y = 0.904x \pm 0.538 + 0.186 \pm 0.030$ Period B $y = 0.388x \pm 0.410 + 0.106 \pm 0.024$
7d	Period A $y = -0.053x \pm 0.365 + 0.241 \pm 0.029$ Period B $y = 0.918x \pm 0.252 + 0.062 \pm 0.018$
7e	Period A $y = 0.001x \pm 0.003 + 0.229 \pm 0.019$ Period B $y = 0.005x \pm 0.004 + 0.114 \pm 0.013$
7f	Period A $y = 0.006x \pm 0.003 + 0.193 \pm 0.029$ Period B $y = -0.004x \pm 0.005 + 0.136 \pm 0.013$
9a	$y = 4.351x \pm 0.874 + 2.648 \pm 0.281$
9b	$y = 0.418x \pm 0.535 + 1.432 \pm 0.173$
9c	$y = 1.245x \pm 0.103 + 1.526 \pm 0.209$
9d	$y = 9.168x \pm 10.900 + 1.499 \pm 0.138$
9e	$y = 0.248x \pm 0.236 + 3.572 \pm 0.378$
9f	$y = 0.399x \pm 0.328 + 1.373 \pm 0.166$
9g	$y = -0.256x \pm 0.312 + 4.138 \pm 0.292$
9h	$y = 1.165x \pm 0.166 + 0.625 \pm 0.140$

Evidence for ambient dark aqueous SOA formation in the Po Valley, Italy

A. P. Sullivan et al.

Title Page

Abstract Introduction

Conclusions References

Tables Figures

◀ ▶

◀ ▶

Back Close

Full Screen / Esc

Printer-friendly Version

Interactive Discussion



Evidence for ambient dark aqueous SOA formation in the Po Valley, Italy

A. P. Sullivan et al.

Title Page

Abstract

Introduction

Conclusions

References

Tables

Figures



Back

Close

Full Screen / Esc

Printer-friendly Version

Interactive Discussion



Table 3. Parameters of the multilinear regression analysis of WSOC. Slope coefficients are reported for the individual AMS ME-2 factors, while y -intercepts are presented in the right column. Numbers in parenthesis refer to the percent contributions of each AMS factors (and of intercepts) to the measured WSOC. See the main text for further explanation.

		OOA-1	OOA-2	OOA-3	OOA-4	Intercept
Whole campaign	intercept forced to 0	0.56 (7%)	0.87 (12%)	0.83 (32%)	1.00 (49%)	–
	unforced	0.40 (5%)	0.94 (12%)	0.63 (24%)	0.92 (44%)	0.31 μgCm^3 (15%)
Period A	intercept forced to 0	1.00 (7%)	0.88 (37%)	0.77 (32%)	1.00 (24%)	–
	unforced	0.88 (6%)	0.92 (38%)	0.48 (19%)	0.59 (14%)	0.72 μgCm^3 (22%)
Period B	intercept forced to 0	0.83 (11%)	1.00 (1%)	0.93 (32%)	1.00 (56%)	–
	unforced	0.27 (4%)	1.00 (1%)	0.46 (15%)	1.00 (53%)	0.47 μgCm^3 (28%)

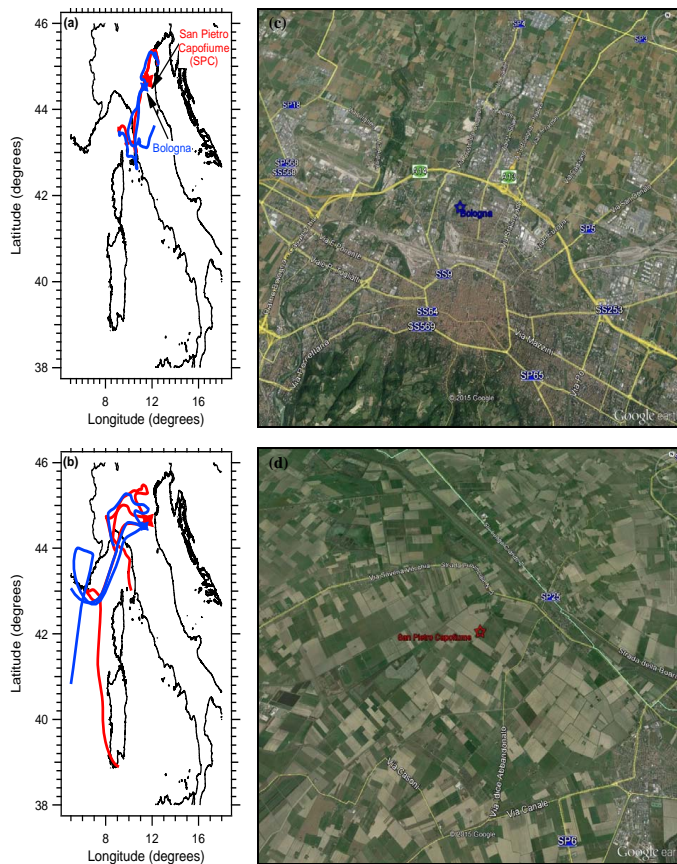


Figure 1. Left panel: characteristic 72 h air mass back trajectories for (a) Period A and (b) Period B at the PEGASOS ground sites of Bologna and SPC. All back trajectories are based on the NOAA ARL HYSPLIT trajectory model. Right panel: maps created using Google Earth (version 7.1.5.1557) to show the areas surrounding the (c) Bologna and (d) SPC sampling sites.

Evidence for ambient dark aqueous SOA formation in the Po Valley, Italy

A. P. Sullivan et al.

Title Page

Abstract

Introduction

Conclusions

References

Tables

Figures

◀

▶

◀

▶

Back

Close

Full Screen / Esc

Printer-friendly Version

Interactive Discussion



Evidence for ambient dark aqueous SOA formation in the Po Valley, Italy

A. P. Sullivan et al.

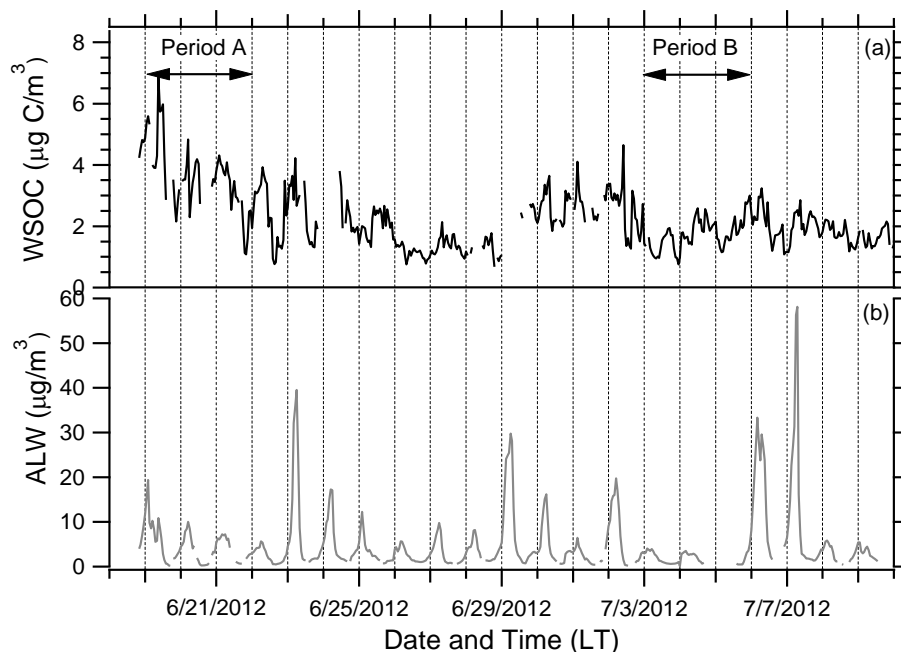


Figure 2. Times series of hourly averaged measured (a) WSOC and (b) calculated ALW at SPC. The dashed vertical lines indicate midnight local time (UTC + 2). Periods A and B are also indicated.

[Title Page](#)[Abstract](#)[Introduction](#)[Conclusions](#)[References](#)[Tables](#)[Figures](#)[◀](#)[▶](#)[◀](#)[▶](#)[Back](#)[Close](#)[Full Screen / Esc](#)[Printer-friendly Version](#)[Interactive Discussion](#)

Evidence for ambient dark aqueous SOA formation in the Po Valley, Italy

A. P. Sullivan et al.

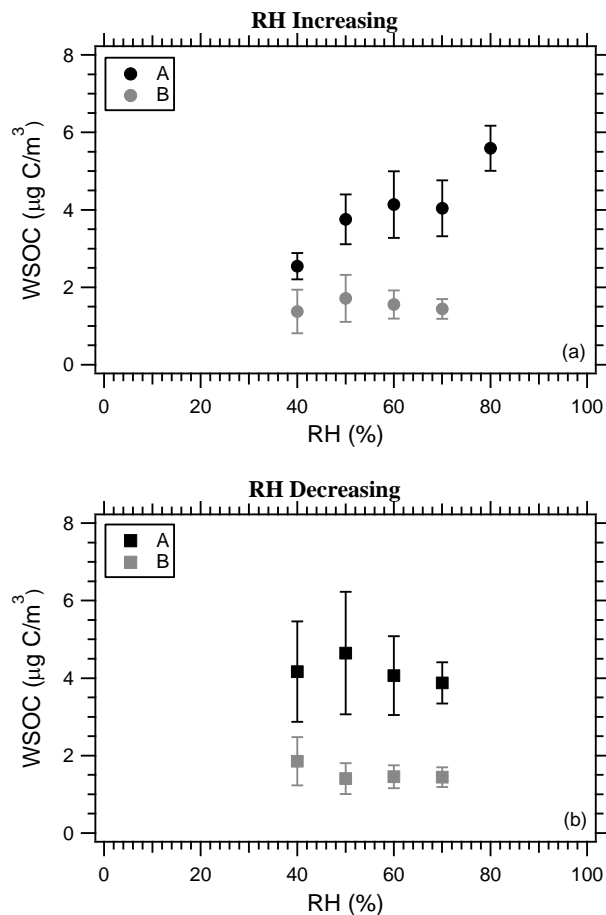


Figure 3. Hourly averaged WSOC as a function of RH for Periods A and B during the times of RH (a) increasing and (b) decreasing at SPC. The WSOC was binned into 10% RH bands starting at 40% RH. The error bars represent the standard deviation at each bin.

Evidence for ambient dark aqueous SOA formation in the Po Valley, Italy

A. P. Sullivan et al.

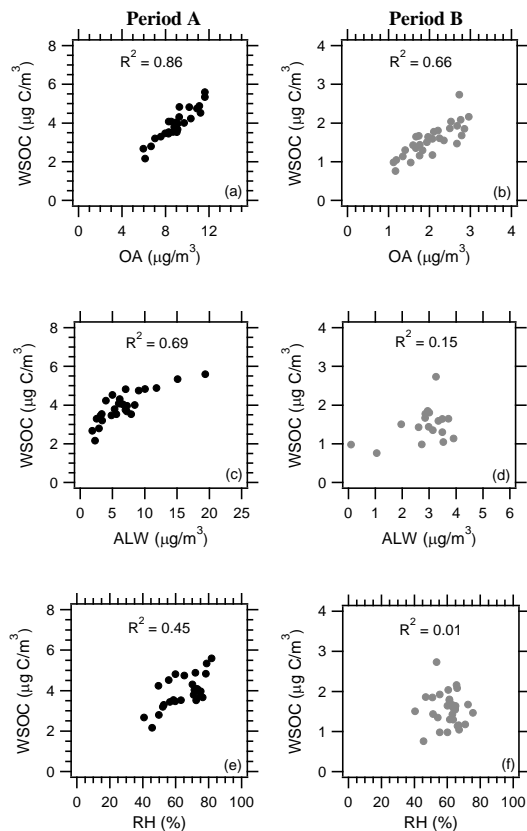


Figure 4. Correlation of hourly averaged WSOC vs. OA for (a) Period A and (b) Period B, ALW for (c) Period A and (d) Period B, and RH for (e) Period A and (f) Period B at SPC. All plots are for during the times of RH increasing.

[Title Page](#)[Abstract](#)[Introduction](#)[Conclusions](#)[References](#)[Tables](#)[Figures](#)[◀](#)[▶](#)[◀](#)[▶](#)[Back](#)[Close](#)[Full Screen / Esc](#)[Printer-friendly Version](#)[Interactive Discussion](#)

Evidence for ambient dark aqueous SOA formation in the Po Valley, Italy

A. P. Sullivan et al.

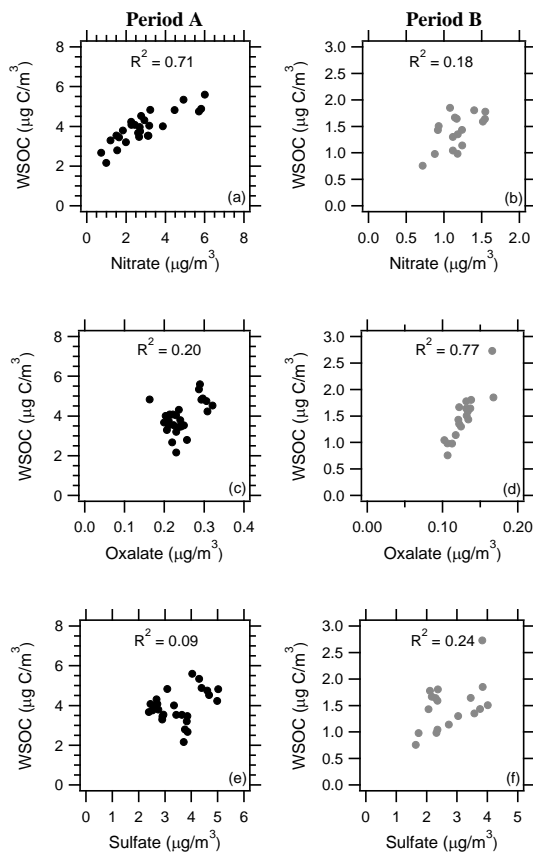


Figure 5. Correlation of hourly averaged WSOC vs. nitrate for (a) Period A and (b) Period B, oxalate for (c) Period A and (d) Period B, and sulfate for (e) Period A and (f) Period B at SPC. All plots are for during the times of RH increasing.

[Title Page](#)[Abstract](#)[Introduction](#)[Conclusions](#)[References](#)[Tables](#)[Figures](#)[◀](#)[▶](#)[◀](#)[▶](#)[Back](#)[Close](#)[Full Screen / Esc](#)[Printer-friendly Version](#)[Interactive Discussion](#)

Evidence for ambient dark aqueous SOA formation in the Po Valley, Italy

A. P. Sullivan et al.

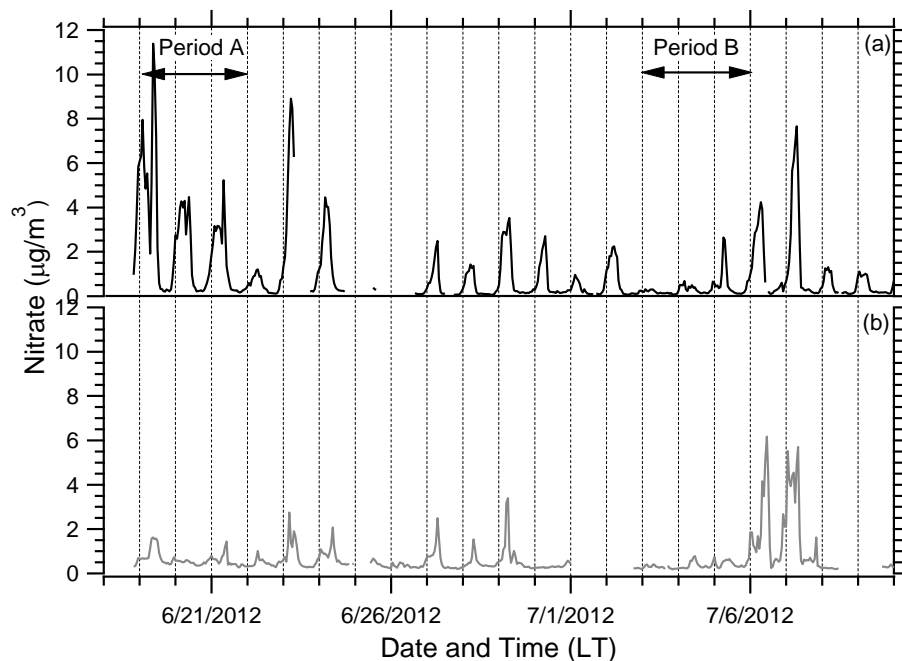


Figure 6. Times series of hourly averaged AMS nitrate observed at **(a)** SPC and **(b)** Bologna. The dashed vertical lines indicate midnight local time (UTC + 2). Periods A and B are also indicated.

[Title Page](#)[Abstract](#)[Introduction](#)[Conclusions](#)[References](#)[Tables](#)[Figures](#)[◀](#)[▶](#)[◀](#)[▶](#)[Back](#)[Close](#)[Full Screen / Esc](#)[Printer-friendly Version](#)[Interactive Discussion](#)

Evidence for ambient dark aqueous SOA formation in the Po Valley, Italy

A. P. Sullivan et al.

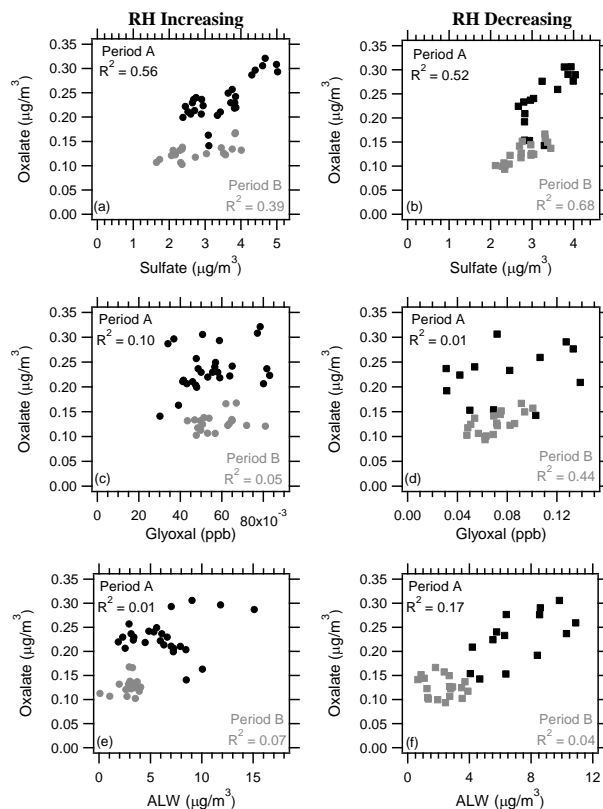


Figure 7. Correlation of hourly averaged oxalate vs. sulfate for Period A and Period B during the times of RH (a) increasing and (b) decreasing, gas-phase glyoxal for Periods A and B during the times of RH (c) increasing and (d) decreasing, and ALW for Periods A and B during the times of RH (e) increasing and (f) decreasing at SPC.

Title Page

Abstract

Introduction

Conclusions

References

Tables

Figures



Back

Close

Full Screen / Esc

Printer-friendly Version

Interactive Discussion



Evidence for ambient dark aqueous SOA formation in the Po Valley, Italy

A. P. Sullivan et al.

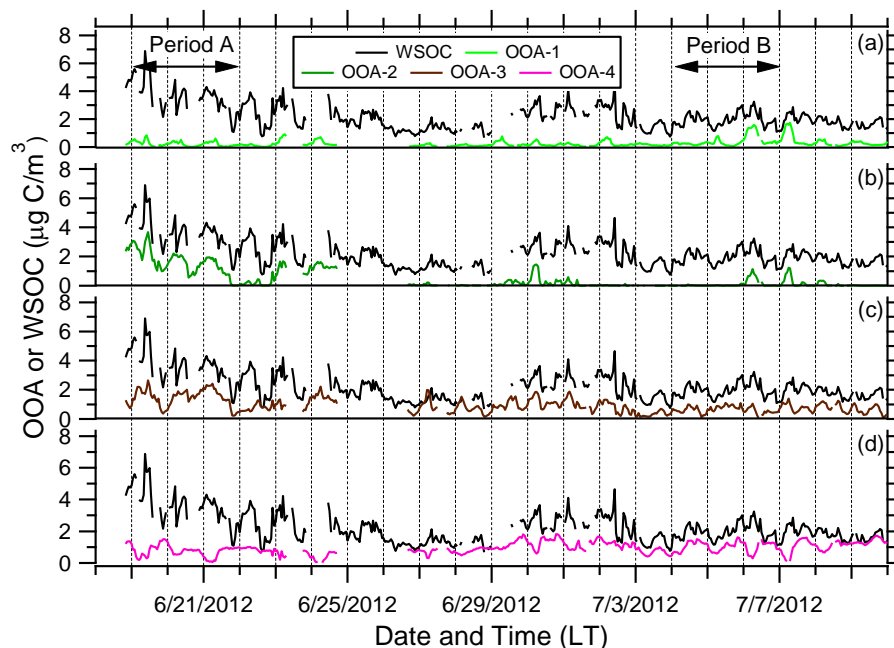


Figure 8. Times series of hourly averaged WSOC with AMS ME-2 factors **(a)** OOA-1, **(b)** OOA-2, **(c)** OOA-3, and **(d)** OOA-4 at SPC. The units for each factor have been converted from $\mu\text{g m}^{-3}$ to $\mu\text{g C m}^{-3}$ using their calculated OM/OC ratio (OOA-1 = 1.81, OOA-2 = 2.15, OOA-3 = 2.13, and OOA-4 = 1.62). The dashed vertical lines indicate midnight local time (UTC + 2). Periods A and B are also indicated.

Title Page

Abstract

Introduction

Conclusions

References

Tables

Figures



Back

Close

Full Screen / Esc

Printer-friendly Version

Interactive Discussion



Evidence for ambient dark aqueous SOA formation in the Po Valley, Italy

A. P. Sullivan et al.

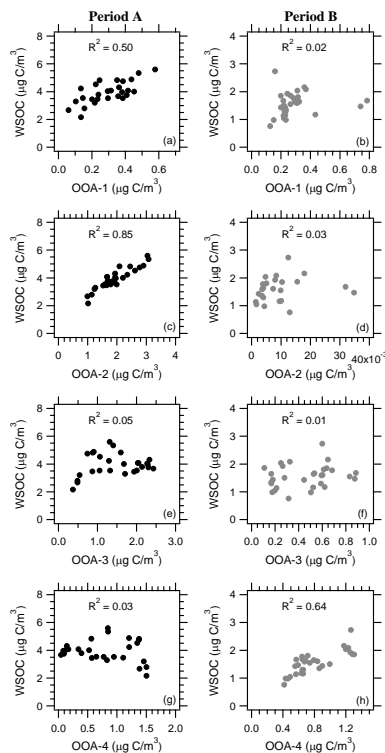


Figure 9. Correlation of hourly averaged WSOC vs. AMS ME-2 factors OOA-1 for **(a)** Period A and **(b)** Period B, OOA-2 for **(c)** Period A and **(d)** Period B, OOA-3 for **(e)** Period A and **(f)** Period B, and OOA-4 for **(g)** Period A and **(h)** Period B at SPC. All plots are for during the times of RH increasing.

Evidence for ambient dark aqueous SOA formation in the Po Valley, Italy

A. P. Sullivan et al.

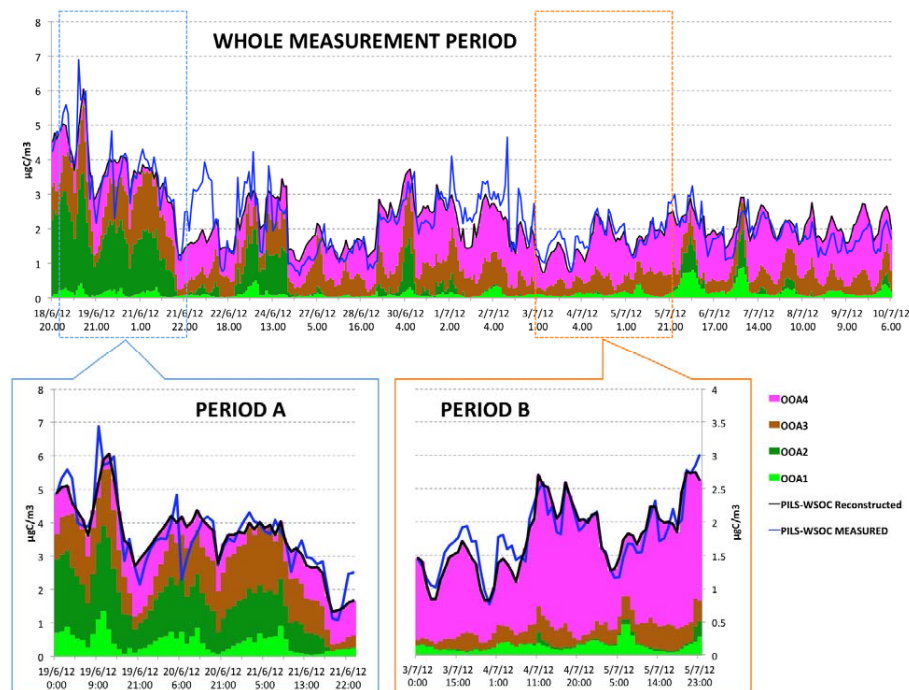


Figure 10. Time series of hourly averaged AMS ME-2 OOA factors, WSOC measured, and WSOC reconstructed for the whole measurement period (top), Period A (bottom left), and Period B (bottom right) at SPC. The units for each OOA factor have been converted from $\mu\text{g m}^{-3}$ to $\mu\text{g C m}^{-3}$ using their calculated OM/OC ratio.

Title Page

Abstract

Introduction

Conclusions

References

Tables

Figures



Back

Close

Full Screen / Esc

Printer-friendly Version

Interactive Discussion



Evidence for ambient dark aqueous SOA formation in the Po Valley, Italy

A. P. Sullivan et al.

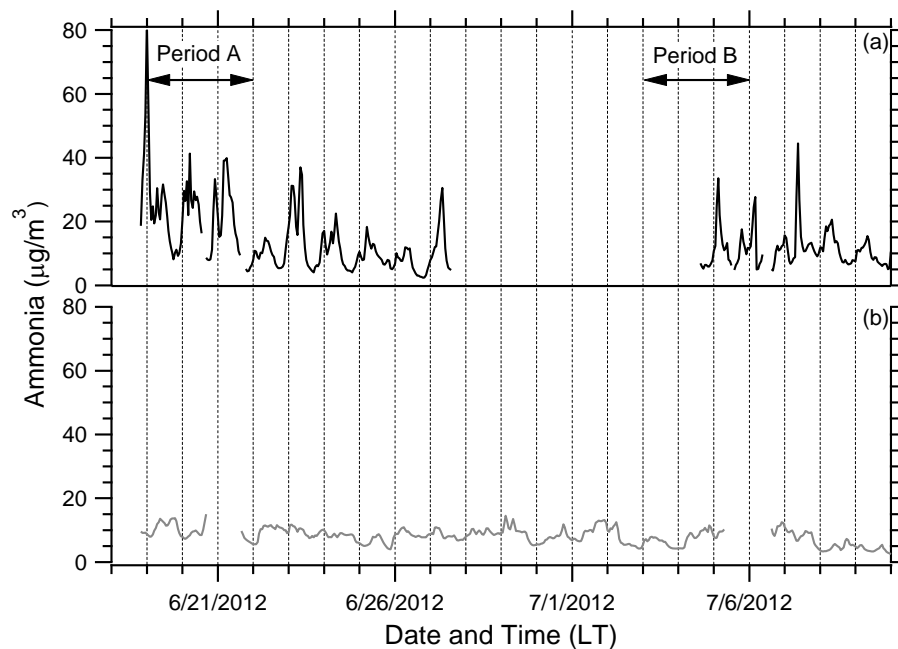


Figure 11. Times series of hourly averaged ammonia observed at **(a)** SPC and **(b)** Bologna. The dashed lines indicate midnight local time (UTC + 2). Period A and Period B are also indicated.

[Title Page](#)[Abstract](#)[Introduction](#)[Conclusions](#)[References](#)[Tables](#)[Figures](#)[◀](#)[▶](#)[◀](#)[▶](#)[Back](#)[Close](#)[Full Screen / Esc](#)[Printer-friendly Version](#)[Interactive Discussion](#)